High Pressure Hydrogen Attack of Steel

J. R. THYGESON, JR.[1] and M. C. MOLSTAD
University of Pennsylvania, Philadelphia, Pa.

Rates of attack of carbon steel and alloy steel by hydrogen at temperatures of 400° and 500° C. and pressures ranging from 340 to 1000 atm. were measured. The influences of exposure time, temperature, pressure, stress, carbon content, microstructure, and alloying elements on the rate of attack were investigated in order to gain insight into the mechanism of the process. The criteria of attack were the extent of damage to the microstructure as determined by metallographic examination, changes in mechanical properties, loss of carbon, and volume change of the specimen. The attack process was characterized by a temperature-dependent induction period followed by a period of rapid attack accompanied by extensive decarburization and structural damage. The final stage of the process was described by a slow rate of change of strength properties and carbon content, with no appreciable increase in structural damage. Mechanisms for the process were postulated, and the rate-determining steps were ascertained.

ALTHOUGH THE deleterious effect of hydrogen in steel has long been recognized there has been little quantitative study of the reaction of high-pressure, high-temperature hydrogen gas with carbon steel and alloy steel. Moreover, the nature of the reaction is dependent upon the temperature, pressure, moisture content of the hydrogen, and other variables that have often been unrecognized and uncontrolled.

At room temperature and at pressures above about 2000 atm. dry hydrogen will effectively embrittle steel without permanent damage to the microstructure (*15*). The degree of reversible embrittlement is a function of the hydrogen pressure, exposure time, exposure temperature, and chemical composition of the steel. In general, austenitic steels are much less susceptible to embrittlement than are ferritic steels. The resistance of the stainless steels to embrittlement is attibuted to the presence of a surface layer of chromium oxide (*10*). It is significant, however, that the diffusivity of hydrogen in austenitic steel is considerably less than its diffusivity in ferritic steel (*5*).

Hydrogen attack of steel is characterized by permanent damage to the microstructure, as evidenced by fissures and enlarged grain boundaries, and by decarburization. This deterioration of the metal causes a marked reduction in both strength and ductility. Hydrogen attack of carbon steel is significant at temperatures above 200° C. and up to the transformation temperature, and at pressures above 25 atm. Below 200° C. it is unlikely that this phenomenon will occur at any pressure (*15*). As the temperature increases, the pressure for the initiation of attack decreases. Nelson presents graphically an approximate relationship between hydrogen temperature and pressure for significant attack with the composition of the steel as a parameter (*8*).

The hydrogen attack of steel is attributed to the reaction of carbon, at grain boundaries and other sites of high interfacial energy, with hydrogen, diffusing to these sites, to form methane. Since the methane molecule cannot diffuse interstitially through the metal lattice, the accumulation of methane under high pressure at reaction sites may eventually lead to grain boundary fissuring. Podgurski (*11*) recently collected and analyzed the gas contained in voids of hydrogen-saturated steel and found this to consist primarily of methane. Also, the quantity of methane formed was in accord with the amount of carbon removed from the steel.

[1] Present address: Drexel Institute of Technology, Philadelphia, Pa.

Although the attack of carbon steel by gaseous hydrogen at high temperature has been well explored in the low pressure region (*1, 17*), Naumann's work (*7*) presents most of the fundamental data available for pressures above 200 atm. The lack of knowledge of the attack process at elevated pressures is emphasized by the numerous reports in the literature of the structural failure of process equipment in high-pressure, high-temperature hydrogen service (*3, 4, 8, 9, 16*). In each case progressive hydrogen attack as evidenced by decarburization and fissure formation was observed in the carbon steel parts exposed to the gas.

The purpose of the present investigation was to determine the phenomenological aspects of hydrogen attack of steel at high pressures. Of particular interest was the influence of exposure time, hydrogen pressure and temperature, and the metal microstructure, chemical composition, and mechanical stress on the extent and rate of hydrogen attack of steel.

Since any proposed mechanism of the attack process must consider the carbon-hydrogen reaction within the steel, the progressive change in carbon content was measured quantitatively and related to the corresponding change in the mechanical properties as determined by the tensile-test.

EXPERIMENTAL PROCEDURE

The steels used in this work were selected on the basis of their commercial availability and their application to equipment subject to exposure to hydrogen at high temperature and high pressure. Nelson's graphical correlation was a useful guide in this respect. The steels and chemical compositions are given in Table I.

Except for two specimens of AISI-C1095 steel which were normalized (one hour at 900° C.), the steels were not heat treated after the machining operation.

The following test specimens were used: tensile-test vessels, Figure I; thick-walled cylinders—$\frac{3}{8}$ inch O.D., $\frac{3}{32}$ inch I.D., 2 inches long; wires—$\frac{1}{16}$ inch diameter, 2-$\frac{7}{8}$ inches long, with a $\frac{3}{8}$ inch gage length, 0.06 inch diameter. The tensile-test specimen, similar to that used by Van Ness (*15*), formed a miniature pressure vessel containing the high pressure hydrogen. Nine of these specimens were mounted in an electrically-heated, temperature-controlled furnace (*14*). Static exposure conditions were maintained. In some cases, a single wire specimen was placed in the axial hole of the tensile-test vessel to determine if absence of mechanical stress affected the attack.

Table I. Chemical Composition of Test Materials

Steel	Composition, wt. %	Condition
C-1010	Nominal: 0.10 C, 0.40 Mn, 0.04 P, 0.05 S	As received (Annealed)
C-1095	Nominal: 0.95 C, 0.40 Mn, 0.04 P, 0.05 S	As received (Spheroidized)
2Cr-1Mo	0.10 C, 0.42 Mn, 0.012 P, 0.022 S, 0.33 Si, 2.08 Cr, 0.96 Mo	As received (Forged)
502	0.09 C, 0.50 Mn, 0.22, P, 0.014 S, 0.39 Si, 5.17 Cr, 0.55 Mo	As received (Forged)
A-286	0.05 C, 1.35 Mn, 0.50 Si, 15 Cr, 26 Ni, Mo, 2.0 Ti	As received (Solution treated)
16-25-6	0.08 C, 1.35 Mn, 0.70 Si, 16 Cr, 25 Ni, 6.0 Mo	As received (Annealed)
19-9 DL	0.30 C, 1.10 Mn, 0.60 Si, 19 Cr, 9.0 Ni, 1.25 Mo, 1.2 W, 0.40 Cb, 0.30 Ti	As received (Annealed)

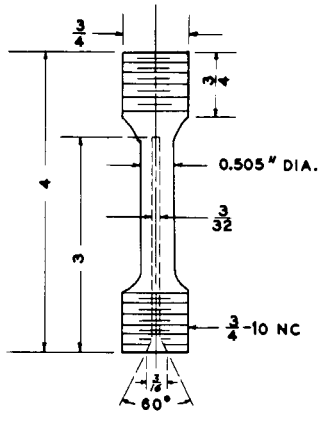

Figure 1. Tensile-test vessel

Cylinders and wires were exposed to the hydrogen in a test tube reactor measuring 7/16 inch I.D. by 12-inches inside length. The reactor was mounted in a small combustion-tube furnace in which the temperature was controlled manually.

In the exposure tests, the hydrogen pressure ranged from 340 to 1000 atm. at temperatures of 400° to 500° C. Commercial hydrogen was compressed from cylinder pressure (150 atm.) to test pressure in an Autoclave Engineers high-pressure pump and stainless-steel-lined compression cylinder assembly (*14*), and supplied to the reactors through a high-pressure distribution system, Figure 2.

Subsequent to exposure to hydrogen, several specimens, after cooling, were immediately subjected to a room temperature tensile test by means of the Instron machine. A cross-head speed of 0.01 inch per minute was used. Other specimens, after exposure, were aged at room temperature for several weeks or given a low-temperature heat-treatment (400° C. for 48 hours). This was done to separate the effect of reversible physical embrittlement from that of attack, as observed in the tensile test.

RESULTS AND DISCUSSION

The extent of attack as a function of exposure time was determined to relate the rate of the process to the variables of time, temperature, pressure, stress condition, carbon content, microstructure, and the concentration of alloying elements.

Index of Hydrogen Attack. The extent of attack in the specimens was measured from the ultimate strength and strain to fracture as obtained from the tensile test, volume change of specimen, carbon content obtained from carbon analysis, and metallographic examination of the microstructure. Normally, more than one index was used to

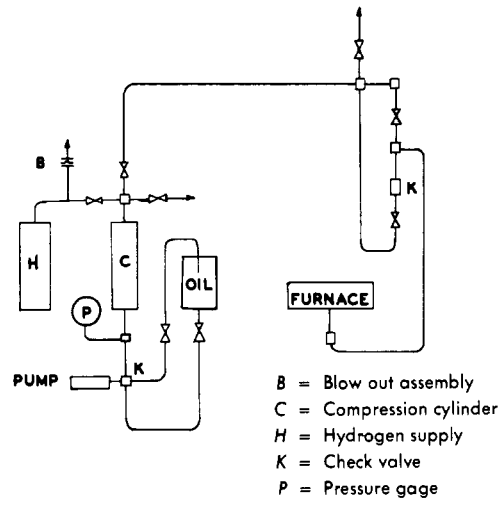

Figure 2. High pressure distribution system

evaluate the extent of attack. This reduced the probability of error resulting from inconclusive data obtained by one method of observation.

Volume change of wire and cylindrical specimens was determined by measuring the length and the diameter at several random points, along the longitudinal axis and around the circumference, and averaging the micrometer readings. Carbon content was determined by heating approximately 1.5 grams of the finely divided sample in oxygen at 1000° C. in an electric combustion-tube furnace. The CO_2 formed by combustion was recovered in soda-lime, and the amount of carbon was obtained by measuring the increase in weight of the absorption tube.

In several of the exposure tests on the wire specimens, triplicates were used. In terms of per cent of volume change the standard deviation was about 0.60% when the mean volume change was approximately 15%. The standard deviation of ultimate strength data in the cases where triplicates were tested was about 5% of the mean value. Only one specimen for a given exposure condition was used in the case of the cylindrical specimens. Because these specimens were considerably larger than the wire specimens, greater reliability could be placed on the results of individual runs.

An attempt was made to correlate weight loss of the wire specimen with carbon loss; however, in the majority of the tests, the loss in weight was less than that corresponding to the reduction in carbon content as determined by carbon analysis. Residual methane trapped in voids and subsequently released after the specimen had been broken into chips probably accounts for this discrepancy. Furthermore, since the specimens were cooled in air after removal from the furnace, any surface oxidation could lead to error because of the high surface to volume ratio and the small size of the specimen.

The correlation of ultimate strength of the wire specimens, after exposure to hydrogen, with residual carbon content is shown in Figure 3 for AISI 1095 steel. For both the high-carbon and low-carbon steels this property was found to be a more sensitive indicator of attack than either the yield strength or the reduction in area. Strain to fracture, as obtained in the tensile test, proved an unreliable measure of attack unless compared with some other indicator such as carbon loss or reduction in ultimate strength.

The progress of attack could also be followed by measuring the increase in volume of the specimen with time of exposure. In every case of pronounced decarburization, the accompanying volume change could be correlated with the change in carbon content. This is shown in Figure 4

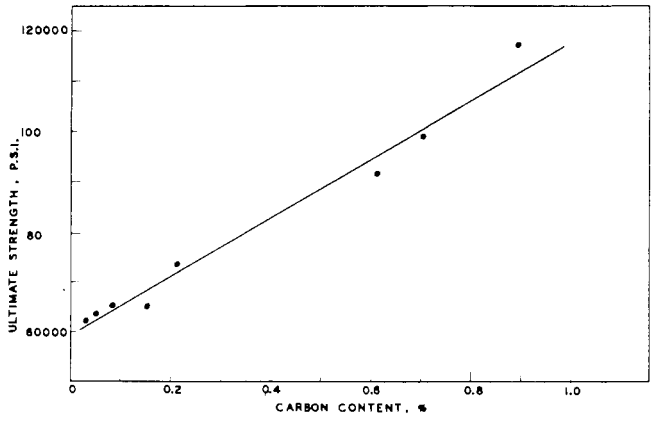

Figure 3. Ultimate strength as a function of residual carbon content for attacked AISI-C1095 wire specimens

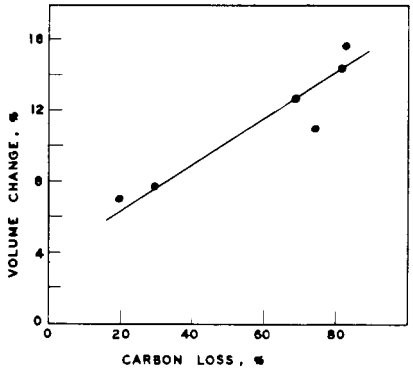

Figure 4. Volume change versus carbon loss for attacked AISI-C1095 wire specimens

for the wire specimens of AISI 1095 steel. Thick-walled cylinders of the same steel showed a parabolic relationship between volume change and time of exposure (Figure 5). Because the exposure times were insufficient to allow attack to penetrate throughout the cross-section of the cylinder, the precent volume changes for these specimens were smaller than those for the completely attacked wires. For all specimens and exposure conditions, no measurable volume change occurred during the initial induction period or the final period of low rate of attack, indicating that fissure growth was negligible in these periods. The approximately linear relationship between the volume change and carbon loss over the greater part of the decarburization range, Figure 4, indicates that the fissure producing agent is methane rather than molecular hydrogen. In no case was the increase in volume reduced by subsequent heating of the specimen in air at 400° C. thereby demonstrating that irreversible structural damage had occurred.

Effect of Exposure Time and Temperature. The pattern of hydrogen attack at temperatures of 400° and 500° C. and at a hydrogen pressure of 1000 atm. is shown in Figures 6 and 7 for a spheroidized steel wire of 0.95% initial carbon content. In terms of changes in ultimate strength (Figure 6) and carbon content (Figure 7) the attack process is characterized by three sharply demarcated periods, namely, the induction period, the period of maximum attack rate, and the final period of low attack rate. The first two periods were temperature dependent, whereas the final period appeared to be little affected by temperature. No changes in the tensile-test properties or the carbon content were observed during the induction period. The microstructure was also uneffected (Figure 8). Once attack began, however, rapid decarburization (Figure 7) accompanied by severe damage to the microstructure (Figure 9) took place. During this period, the formation and growth of internal

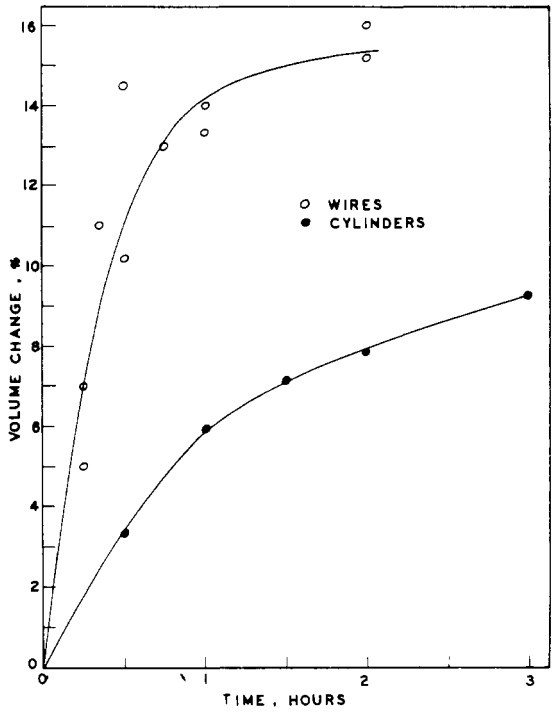

Figure 5. Volume change as a function of exposure time for AISI-C1095 steel exposed to hydrogen at 500° C. and 1000 atm.

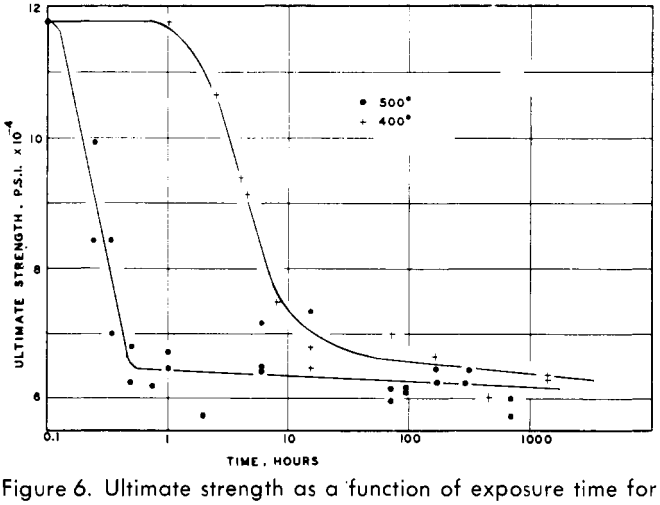

Figure 6. Ultimate strength as a function of exposure time for AISI-C1095 wire specimens exposed to hydrogen at 1000 atm.

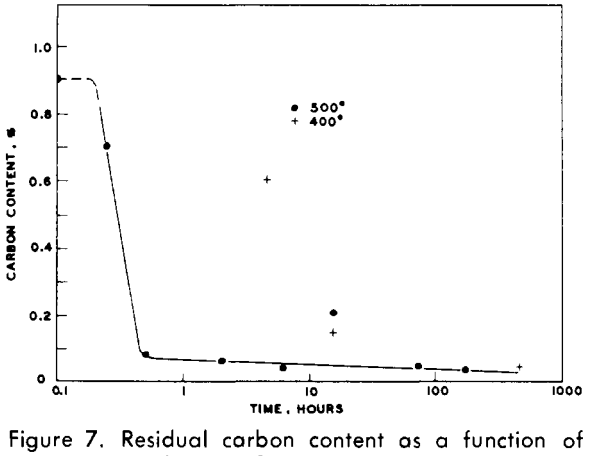

Figure 7. Residual carbon content as a function of exposure time for AISI-C1095 wire specimens exposed to hydrogen at 500° C. and 1000 atm.

fissures accounted for the time-dependent nature of the process. The permanent damage to the metal caused a drastic reduction in the strength properties and a loss of ductility. Fissures propagated in a ductile manner and appeared to follow prior austenitic grain boundaries.

In the final period, further growth of fissures was negligible; consequently, little change of the properties of the steel with time was observed. Since the rate of propagation of a fissure is dependent on both the temperature and pressure of the entrapped methane, the availability to the reaction zone of carbon in the form of Fe_3C is necessary to maintain the progress of attack. In the final period of the process, carbon has been depleted to such an extent that virtually no methane is formed to maintain the fissure growth rate. Consequently, further reduction in the strength properties of the specimen is only affected by the creep characteristics of the metal under the internal methane pressure.

An experimental estimate of the activation energy for attack in the period of maximum rate gives a value of 33 kcal. This quantity is determined by the contributions of the activation energies for the individual steps making up the attack process. The steps include adsorption and dissociation of hydrogen molecules at the gas-metal interface, diffusion of hydrogen and carbon atoms to the reaction site, formation of methane, dissolution of carbide in the ferrite matrix to replenish the supply of carbon atoms, and creation of new reaction surface by the growth of fissures. Since the activation energies for the diffusion of hydrogen and carbon atoms in steel are approximately 3 and 18 kcal., respectively, neither of these processes appears to be rate-controlling. Schenck and Taxhet (*13*) report a range of 12 to 16.2 kcal. for the activation energy of surface processes in the permeation of steel by hydrogen, indicating that this step also is probably not controlling. However, Allen and coworkers (*1*) suggest that at much lower pressures (27 to 95 atm.) a surface-controlled mechanism is dominant in the attack of annealed SAE 1020 steel.

Effect of Hydrogen Pressure. The influence of hydrogen pressure on the rate of attack of AISI-1095 steel at 500° C. is shown in Figure 10. For the three pressures investigated (340, 680, and 1000 atm.) the criterion of attack was the per cent increase in volume of the specimen after an exposure time of one hour.

The important conclusions to be derived from these data are the existence of a pressure dependence of the attack process, and the clear indication that the diffusion of hydrogen or carbon atoms is not the rate-controlling step. One would expect a negligible effect of hydrogen pressure if the diffusion of carbon atoms or the dissolution of carbide were the dominant mechanisms in the attack process. Furthermore, the diffusion of hydrogen atoms as the controlling step is unlikely since the per cent volume change varies more nearly as the square of the pressure than as the square root. (For simple interstitial diffusion of hydrogen atoms through steel, Richardson (*12*) has shown that the rate of diffusion is proportional to the square root of the hydrogen pressure.)

The results of the present investigation indicate, therefore, that the attack process is not controlled by either carbon diffusion or hydrogen permeation but probably by the chemical reactions leading to the formation of methane. The magnitude of the pressure effect and of the experimentally estimated energy of activation strongly supports this hypothesis.

The effect of pressure on the extent of damage to the microstructure is clearly illustrated by Figures *9*, *11*, and *12* which are photomicrographs of a transverse section through the specimen at the mid-point. In each case the exposure time was one hour at a temperature of 500° C. Several isolated fissures have formed at 340 atm. (Figure 11). It is noteworthy that attack began within the metal rather

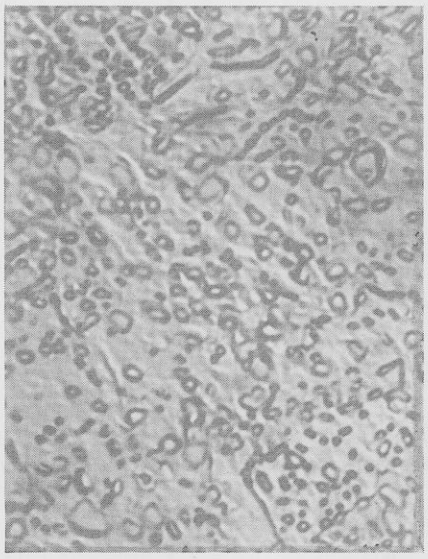

Figure 8. Original microstructure of AISI-C1095 steel
Magnification 1125×

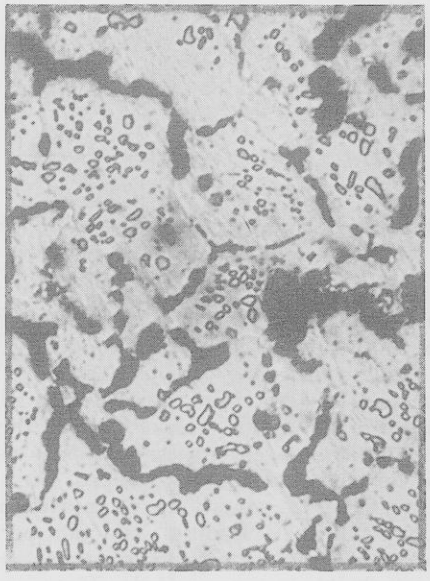

Figure 9. Microstructure of AISI-C1095 steel after one hour exposure to hydrogen at 500° C. and 1000 atm.
Magnification 1125×

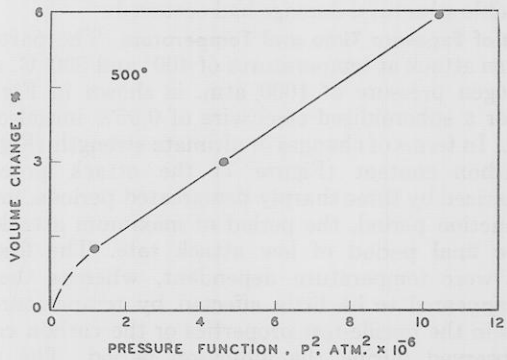

Figure 10. Volume change as a function of the square of the hydrogen pressure for AISI-C1095 cylindrical specimens
Exposure was for one hour at 500° C.

than at the surface. At 680 atm. (Figure 12) a clearly defined network of enlarged grain boundaries has developed. Some spheroidal carbide has disappeared, presumably by dissolution in the surrounding ferrite matrix. Other spheroids have undergone attack, and the voids formed at carbide-ferrite interfaces appear to have coalesced with neighboring reaction sites to form a network of interconnecting fissures. At 1000 atm. (Figure 9) progressive fissure growth has resulted in a random distribution of large voids throughout the region of attack. Much of the carbide has decomposed leaving regions of ferrite adjacent to the fissures.

Effect of Carbon Content. The rate of attack as well as extent of permanent damage to the microstructure were strongly influenced by the initial carbon content of the steel. This is illustrated by comparing Figure 13, in which the ultimate strength is plotted against the exposure time for a 0.10% carbon steel (AISI-C1010), with Figure 6, in which the same variables are plotted for a 0.95% carbon steel (AISI-C1095). In each case the exposure temperatures were 400° and 500° C. at an exposure pressure of 1000 atm.

The predominant effect of the lower carbon content on the attack process was the marked increase in the length of the induction period for both exposure temperatures. Damage to the microstructure caused by the internal methane pressure was small, and only a slight volume change was observed after long exposure times. The relative magnitude of these effects is attributed to the small quantity of methane formed in the process. This amount was insufficient to create the number and size of fissures that are characteristic of attack in high carbon steel. The ductility as measured by the strain to fracture, increased slightly shortly after the initiation of attack. As attack progressed, the ductility decreased, but even after long exposure, it was not greatly reduced. This behavior is similar to that exhibited by surface decarburized steel (Table II). (It is noteworthy that surface decarburization, in contrast to hydrogen attack, does not damage the microstructure because the carbon is removed by interstitial diffusion to the surface rather than by the formation of methane.) No attempt was made here to separate the effect of cold-work on the tensile-test properties from that of attack. Since the "as received" annealed wire (AISI-C1010) was cold-worked in the preparation of the specimens, subsequent recovery and recrystallization taking place during the exposure period and superimposed on the attack process could account for the initial slight increase in ductility. Further work is in progress to determine how cold-working might influence the hydrogen attack of steel.

Effect of Microstructure. For the range of hydrogen temperature and pressure investigated here, the type of microstructure originally present had a significant effect on the rate of attack. This is illustrated by comparing Figure 14, which shows the extent of attack in the spheroidized microstructure after three hours at 500° C. and 1000 atm., with Figure 15, which shows the extent of attack in the pearlitic microstructure after one hour at the same temperature and pressure. For the more stable spheroidized structure the rate of growth of the decarburized zone was 0.23 mm. per hour. This is compared with a rate for the pearlitic specimen of 0.55 mm. per hour.

Archakov (2) similarly found that for a pearlitic steel the rate of decarburization decreased with an increase in the tempering temperature during the prior heat-treatment of the specimen; increasing the tempering temperature caused a corresponding increase in the stability of the carbide phase.

Although the conclusion of this section is based on a single photographic comparison, the difference indicated in the rates of attack of the pearlitic and spheroidal microstructures is great enough to be considered significant. The size of the specimens and the times of exposure were such

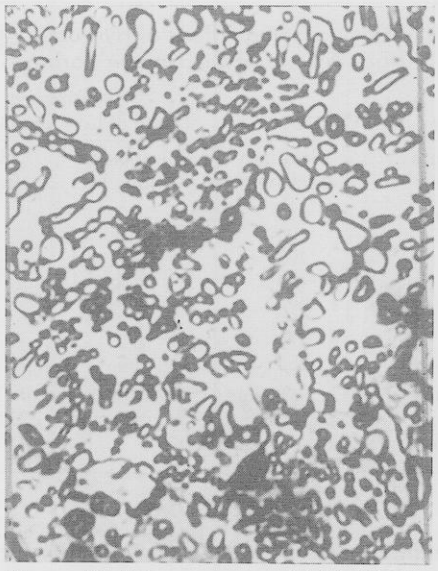

Figure 11. Microstructure of AISI-C1095 steel after one hour exposure to hydrogen at 500° C. and 340 atm.
Magnification 1125×

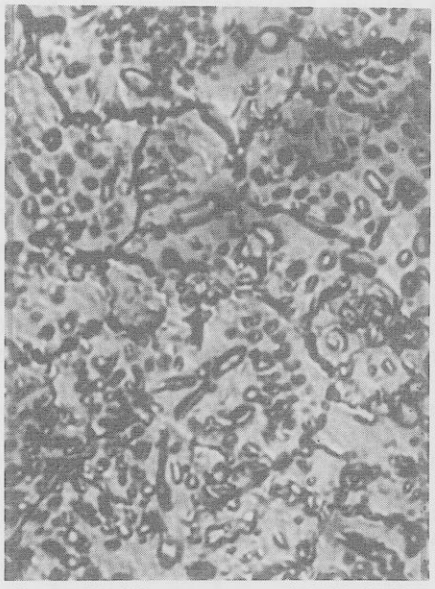

Figure 12. Microstructure of AISI-C1095 steel after one hour exposure to hydrogen at 500° C. and 680 atm.
Magnification 1125×

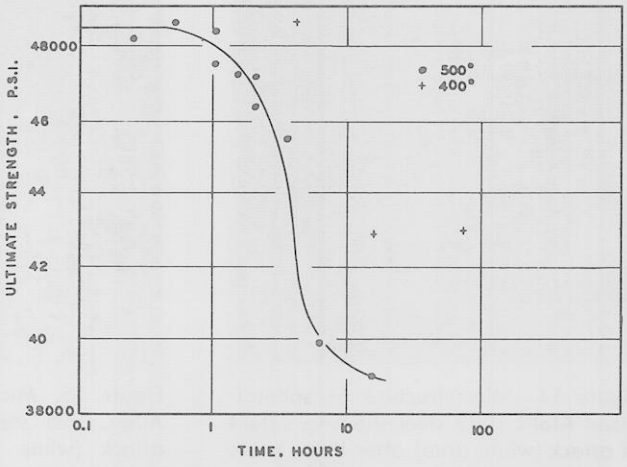

Figure 13. Ultimate strength versus exposure time for AISI-C1010 wire specimens exposed to hydrogen at 1000 atm.

Table II. Comparison of Effects of Hydrogen Attack and Surface Decarburization in Low Carbon Steel

Steel AISI C-1010[a]		Rimmed (Data of Low and Gensamer)[b]	
Exposure time, hr.	Strain to fracture, %	Exposure time, hr.	Strain to fracture, %
0.25	27.7	1.0	24
0.50	29.8	1.4	31
1.0	40.2	1.8	42
1.5	29.0	2.0	44
2.0	40.0	2.4	45
3.5	32.5	2.8	47
6.0	27.8	3.2	46
15.0	25.5	3.6	44

[a] Temperature, 500° C.; pressure, 1000 atm.; water content of hydrogen, nil. [b] Temperature, 710° C.; pressure, 1 atm.; water content of hydrogen, 30% by volume.

Table III. Induction Period for Hydrogen Attack of Alloy Steel[a]

Alloy	Induction Period, Hours
AISI C-1010 (carbon steel)	1
2% chromium-1% molybdenum	1712
502	>2048
A-286	>7020
16-25-6	>7020
19-9 DL	>7020

[a] Exposure conditions: temperature, 500° C.; hydrogen pressure, 1000 atm.; specimen—tensile test.

that a definite pattern of attack in each specimen was established. Moreover, the specimens were prepared from the same piece of bar stock to ensure that the results would not be influenced by variations in chemical composition.

Effect of Alloying Elements. In general, those elements which form carbides of greater thermodynamic stability than that of cementite impart to the steel added resistance to hydrogen attack. An illustration is the effect of the chromium content of the steel on the susceptibility to attack in several alloys of increasing chromium composition. The most distinguishing characteristic of the attack process in these alloys was the prolonged induction period, which increased with an increase in chromium content (Table III). The 2% chromium - 1% molybdenum specimen was the only alloy of those investigated that showed evidence of attack after prolonged exposure to hydrogen at a temperature of 500° C. and a pressure of 1000 atm. As illustrated in the photomicrograph, Figure 16 of a transverse section near the axial hole of the tensile-test specimen, extensive cracking at grain boundaries occurred after an exposure time of 1712 hours.

Effect of Stress. To determine the effect of a stressed condition of the metal on the rate of attack, specimens (AISI-1095) in the form of miniature pressure vessels (Figure 1) were filled with hydrogen at 500° C. and 1000 atm. The stress gradient created through the wall of the specimen by the pressure of the contained gas caused a marked increase in the rate of attack over that occurring in the unstressed specimen for the same hydrogen temperature and pressure. This is indicated by a comparison of Figure 17, which shows the extent of attack (lighter zone extending from the center toward the outer edge) in the stressed specimen after an exposure time of two hours, with Figure 14, showing the extent of attack after 3 hours in the unstressed specimen. A careful measurement of the width of the zone of attack gives an average rate of 0.40 mm. per hour for the stressed specimen as compared to an average rate of 0.23 mm. per hour for the unstressed specimen. After slightly more than three hours, the stressed specimen burst under test as a consequence of the extensive attack.

The recent study of Vitovec and coworkers (*1*) offers corroborative evidence that stress accelerates the rate of attack. The authors suggest that the larger creep strain at higher stresses was the direct cause of the more rapid attack at this stress level than at a lower level. The comparison was made on AISI 1020 steel in the normalized state.

CONCLUSIONS

Ultimate strength as obtained from the tensile test, volume change, and residual carbon content from chemical analysis proved to be sensitive indicators of hydrogen attack in carbon steel. In addition, metallographic examination of the microstructure gave a reliable qualitative estimate of the extent of attack.

The attack process was found to be significantly influenced by temperature, hydrogen pressure, chemical com-

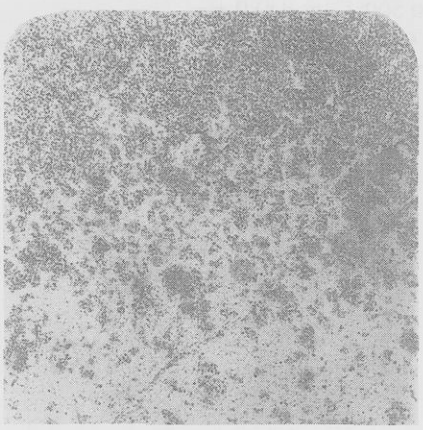

Figure 14. Microstructure of spheroidized AISI-C1095 steel showing extent of attack (white area) after three hours exposure to hydrogen at 500° C. and 1000 atm.
Magnification 150X

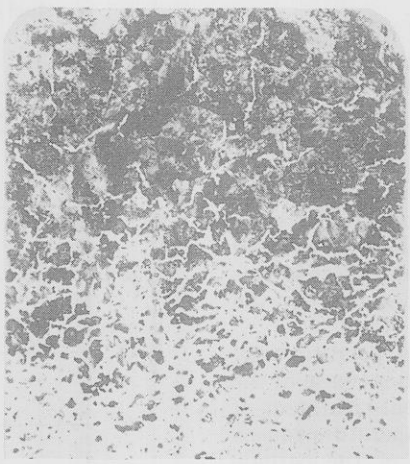

Figure 15. Microstructure of pearlitic AISI-C1095 steel showing extent of attack (white area) after one hour exposure to hydrogen at 500° C. and 1000 atm.
Magnification 150X

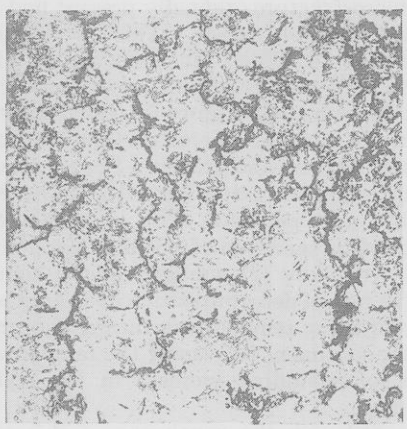

Figure 16. Microstructure of 2% Cr.-1% Mo. steel after 1712 hours of exposure to hydrogen at 500° C. and 1000 atm.
Magnification 150X

position of the steel, microstructure, and stress condition. A characteristic pattern of attack as measured by the above criteria was observed. The chemical reactions leading to the formation of methane were shown to be rate-determining; however, additional data are necessary to substantiate this conclusion.

ACKNOWLEDGMENT

The authors wish to acknowledge the support for one year of Autoclave Engineers Corporation. We also express appreciation to J.J. Monahan of the Midvale-Heppenstal Company for generously providing the carbon analyses of many of the steels tested.

The steels used in this work were donated by United States Steel Corporation, Allegheny Ludlum Steel Corporation, Universal-Cyclops Corporation, and Timken Roller Bearing Company. Testing facilities were made available to us by the School of Metallurgical Engineering, University of Pennsylvania.

LITERATURE CITED

(1) Allen, R.E., Jansen, R.J., Rosenthal, P.C., Vitovec, F.H., *Proc. A.P.I. Sect. III* 41, (1961).
(2) Archakov, Y.I., *Zh. Prikl. Khim.* **33**, 89 (1960).
(3) Ciuffreda, A.R., Rowland, W.D., *Proc. A.P.I., Sect. III* **37**, 116 (1957).
(4) Evans, T.C., *Mech. Eng.* **70**, 414 (1948).
(5) Geller, W., Sun, T.H., *Arch. Eisenhuttenw.* **21**, 423 (1950).
(6) Low, J.R., Gensamer, M., *Trans. AIME* **158**, 207 (1944).
(7) Naumann, F.K., *Stahlu Eisen* **57**, 889 (1937); **58**, 1239 (1938).
(8) Nelson, G.A., *Trans. A.S.M.E.* **73**, 205 (1951).
(9) Nelson, G.A., Effinger, R.T., *Welding J.* N.Y. **34**, 12 (1955).
(10) Perlmutter, D.D., Dodge, B.F., *Ind. Eng. Chem.* **48**, 885 (1956).
(11) Podgurski, H.H., *Trans. AIME* **221**, 389 (1961).

Figure 17. Microstructure of stressed AISI-C1095 steel showing extent of attack (white area) after exposure to hydrogen for 2 hours at 500° and 1000 atm.
Magnification 150×

(12) Richardson, O.W., *Phil. Mag.* **7**, 266 (1904).
(13) Schenck, H., Taxhet, H., *Arch. Eisenhuttenw.* **30**, 661 (1959).
(14) Thygeson, J.R., Ph.D. dissertation, University of Pennsylvania, Philadelphia, Pa., 1961.
(15) Van Ness, H.C., Dodge, B.F., *Chem. Eng. Progr.* **51**, 266 (1955).
(16) Van Rossum, O., *Chem. Ingr. Tech.* **25**, 481 (1953).
(17) Weiner, L.C., *Corrosion* **17**, 137 t (1961).

RECEIVED for review July 2, 1963. Accepted November 7, 1963.